Structure of Surface Tungsten Oxide Species in the WO₃/Al₂O₃ Supported Oxide System from X-ray Absorption Near-Edge Spectroscopy and Raman Spectroscopy

J. A. Horsley,[†] I. E. Wachs,* J. M. Brown, G. H. Via, and F. D. Hardcastle[‡]

Corporate Research Laboratories, Exxon Research and Engineering Company, Annandale, New Jersey 08801 (Received: August 18, 1986)

The X-ray absorption near-edge spectra (XANES) of the L_1 tungsten edge in WO₃/Al₂O₃ samples indicate that the symmetry of the tungsten environment depends on both the surface coverage and the presence of coordinated water. At coverages of less than 1/3 monolayer, in the absence of coordinated water, the XANES spectrum indicates a distorted tetrahedral structure for the surface tungsten oxide species. Samples exposed to air at room temperature have water molecules coordinated to the surface tungsten oxide species and produce an octahedral site symmetry, but the water is removed by heating to 500 °C. The Raman spectra of the WO₃/Al₂O₃ samples are consistent with a distorted tetrahedral tungsten oxide environment and, in addition, show features due to W=O and W–O–W bonds. These results suggest that the surface tungsten oxide is present as both isolated and dimeric tetrahedra. At coverages approaching a monolayer, in the absence of coordinated water, a significant fraction of the surface tungsten oxide sites appears to have a distorted octahedral environment in the XANES spectra. At this high coverage the effect of coordinated water molecules is much less evident than at low coverage. The Raman results, however, only provide information about the tetrahedral component because the Raman cross section of the tetrahedral tungsten oxide is much higher than the octahedral tungsten oxide. The Raman spectra show features of W=O and W–O–W bonds in the tetrahedral fraction of the surface tungsten oxide monolayer on alumina. These observations are consistent with a surface complex where the supported tungsten oxide has formed a polymeric structure on the alumina support composed of WO₄ and WO₆ units jointed in infinite chains.

Introduction

In the alumina-supported tungsten oxide system, WO₃/Al₂O₃, the interaction between tungsten oxide and alumina has a pronounced effect on the properties of the supported tungsten oxide phase. The Raman vibrational bands characteristic of crystalline WO₃ or Al₂(WO₄)₃ are absent in alumina-supported tungsten oxide and, instead, a new set of Raman vibrational bands are observed.[1-8] The alumina-supported tungsten oxide phase is much more difficult to reduce than bulk WO₃ and temperatures several hundred degrees higher than the reduction temperature of bulk WO₃ are required to reduce the supported tungsten oxide phase.[1-5,9-11] These observations have led to the conclusion that below monolayer coverage the supported tungsten oxide phase is present as a highly dispersed and amorphous surface complex coordinated to the alumina support.[1-11] This conclusion is supported by recent in-situ laser Raman studies which revealed that water molecules coordinate to the supported tungsten oxide and perturb its Raman vibrational bands, indicating that the tungsten oxide is indeed present as an atomically dispersed phase on the alumina support surface.[12,13] The WO₃/Al₂O₃ system has been characterized with many different techniques in recent years: temperature-programmed reduction (TPR),[1-5,9-11] laser Raman spectroscopy (LRS),[1-8,12,13] X-ray photoelectron spectroscopy (XPS),[5,9,10] UV–visible diffuse reflectance spectroscopy,[3,4] and X-ray diffraction.[3,4,6-8] However, despite the large amount of work on this system the structure of the alumina-supported surface tungsten oxide complex is still not known. Two different structures have been proposed for the surface tungsten oxide species. One group has proposed that the structure consists of distorted bridged tungstate octahedra,[1,2] while two other groups have proposed a structure consisting of isolated tetrahedral surface complexes.[3-5]

X-ray absorption near-edge spectroscopy (XANES) can provide information on the local symmetry and coordination around a given site. We have studied the surface tungsten oxide coordination in the WO₃/Al₂O₃ system by tungsten L_1-edge XANES. Near-edge spectra for the alumina-supported tungsten oxide species are reported here for the first time. The near-edge structure has enabled us to distinguish between tetrahedral and octahedral

surface tungsten oxide complexes and to obtain information on the role of the coordinated water molecules. Laser Raman spectra of the supported tungsten oxide at various coverages are also reported. The Raman spectra provide additional information about the molecular structure of the supported tungsten oxide species. The combined information from XANES and Raman allows us to monitor the detailed structural changes that occur in the alumina-supported tungsten oxide phase.

Experimental Section

The tungsten oxide on γ-alumina (Engelhard, reforming grade, 180 m²/g) samples were prepared by the incipient wetness impregnation method by adding an aqueous solution of ammonium metatungstate to the alumina powder. The samples were subsequently dried at 110 °C and calcined in air at either 500 or 950 °C for 16 h. Samples containing 2 and 10 wt % WO₃ on γ-alumina were prepared. Previous studies showed that for an alumina support with 180 m²/g monolayer coverage by the surface species is reached at ~30% WO₃ after 500 °C calcination

(1) Thomas, R.; Kerkhof, G. M.; Moulijn, J. A.; Medema, T.; DeBeer, V. H. J. *J. Catal.* **1980**, *61*, 559.
(2) Thomas, R.; DeBeer, V. H. J.; Moulijn, J. A. *Bull. Soc. Chem. Belg.* **1981**, *90*, 1349.
(3) Iannibello, A.; Villa, P. L.; Marengo, S. *Gazz. Chem. Ital.* **1979**, *109*, 5121.
(4) Tiltarelli, P.; Iannibello, A.; Villa, P. L. *J. Solid State Chem.* **1981**, *37*, 95.
(5) Salvati, L.; Makovsky, L. E.; Stencel, J. M.; Brown, F. R.; Hercules, D. M. *J. Phys. Chem.* **1981**, *85*, 3700.
(6) Chan, S. S.; Wachs, I. E.; Murrell, L. L. *J. Catal.* **1984**, *90*, 150.
(7) Chan, S. S.; Wachs, I. E.; Murrell, L. L.; Dispenziere, N. C. *J. Catal.* **1985**, *92*, 1.
(8) Chan, S. S.; Wachs, I. E.; Murrell, L. L.; Dispenziere, N. C. In *Catalysis on the Energy Scene*, Kaliaguine, S., Mahay, A., Eds.; Elsevier: Amsterdam, 1984.
(9) Biloen, P.; Pott, G. T. *J. Catal.* **1973**, *30*, 169.
(10) Wachs, I. E.; Chersich, C. C.; Hardenbergh, J. H. *Appl. Catal.* **1985**, *13*, 335.
(11) Soled, S.; Murrell, L. L.; Wachs, I. E.; McVicker, G. B.; Sherman, L. G.; Chan, S. S.; Dispenziere, N. C.; Baker, R. T. K. In *Solid State Chemistry in Catalysis*, Grasselli, R. K., Brazdil, J. F., Eds.; American Chemical Society: Washington, DC, 1985; ACS Symp. Ser. No. 279, p 165.
(12) Chan, S. S.; Wachs, I. E.; Murrell, L. L. Wang, L.; Hall, W. K. *J. Phys. Chem.* **1984**, *88*, 5831.
(13) Stencel, J. M.; Makovsky, L. E.; Diehl, J. R.; Sarkus, T. A. *J. Raman Spectrosc.* **1984**, *25*, 282.

* Address correspondence to the author at the Department of Chemical Engineering, Lehigh University, Bethlehem, PA 18015.
† Present address: Catalytica Associates, Mountain View, CA 94043.
‡ Present address: Department of Chemistry, Lehigh University, Bethlehem, PA 18015.
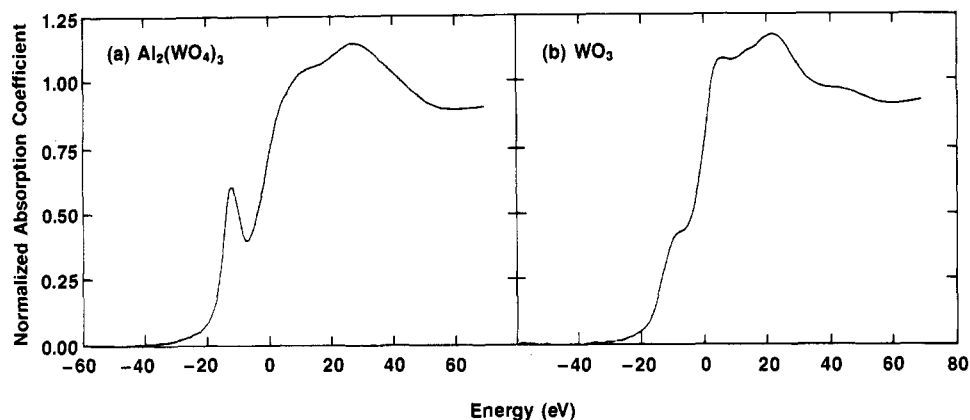
Figure 1. Normalized tungsten L$_1$-edge XANES spectra for the reference compounds (a) Al$_2$(WO$_4$)$_3$ and (b) WO$_3$.

treatment.[5,7,8] The supported tungsten oxide phase in the samples was shown to be present only as a surface species by laser Raman spectroscopy. Samples of pure crystalline WO$_3$, possessing distorted corner-shared octahedra,[14] and pure crystalline Al$_2$(WO$_4$)$_3$, composed of regular and distorted tetrahedral tungstates,[15] were obtained from Cerac. The structures of the WO$_3$ and Al$_2$(WO$_4$)$_3$ samples were confirmed by X-ray diffraction and laser Raman spectroscopy.[6]

The X-ray absorption data were obtained at the Stanford Synchrotron Radiation Laboratory (SSRL) on beamline VII-3 during dedicated operation of SPEAR at 3 GeV and currents of 30–70 mA. Data for air-exposed samples were taken at room temperature by using apparatus designed for transmission and fluorescence X-ray spectroscopy.[16,17] The fluorescence detector was similar to that described by Stern and Heald.[18] Data were also taken on samples after calcination at 500 °C in a mixture of 20% oxygen in helium in order to investigate the effect of removal of the surface-coordinated water. The measurements were carried out in-situ at 500 °C and at room temperature, without exposing the samples to ambient air. For these experiments an in-situ catalyst furnace designed for simultaneous transmission and fluorescence measurements was used.[19]

The energy scale of the XANES spectra were calibrated relative to WO$_3$, using the first derivative of the edge spectrum. The first derivative shows two peaks, the lower energy peak corresponding to the inflection point in the pre-edge feature and the second peak corresponding to the inflection point of the edge itself. The energy scale was set such that the second peak in the derivative spectra corresponded to the W L$_1$ energy (12099.8 eV), and the XANES energies are reported relative to this value. The XANES spectra were normalized by (1) fitting a quadratic polynomial spline to the EXAFS region of the data, (2) fitting a linear function to the pre-edge data, (3) extrapolating both functions to zero energy and taking the difference (the edge step height), and (4) normalizing the data to unit step height.

Laser Raman spectra were obtained with a Spectra-Physics Ar$^+$ laser (Model 2020-05) delivering 1–100-mW incident radiation measured at the sample, where the exciting line was typically 514.5 nm. The scattered radiation was then directed into a Spex Triplemate spectrometer (Model 1877) coupled to a Princeton Applied Research OMA III optical multichannel analyzer (Model 1463) with an intensified photodiode array cooled thermoelectrically to −30 °C. The Raman spectra were recorded with an OMA III dedicated computer and software. The overall resolution

(14) Wells, A. F. *Structural Inorganic Chemistry*; Oxford University: London, 1984.
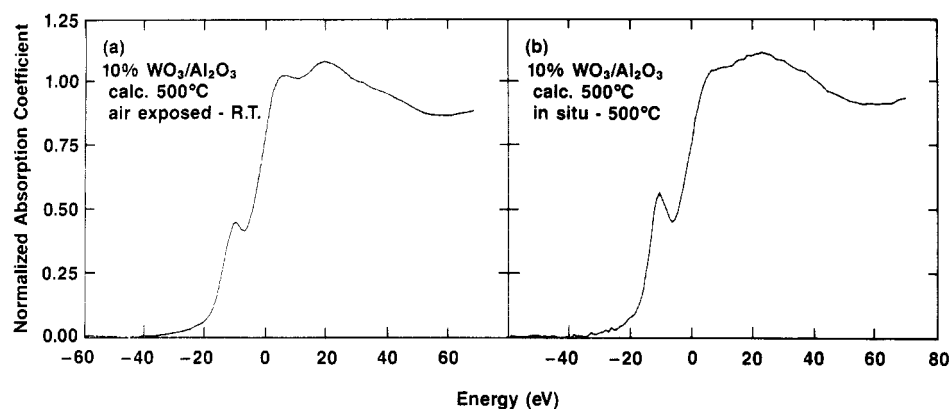(15) Craig, D. C.; Stephenson, N. C. *Acta Crystallogr., Sect. B* **1968**, *B24*, 1250.
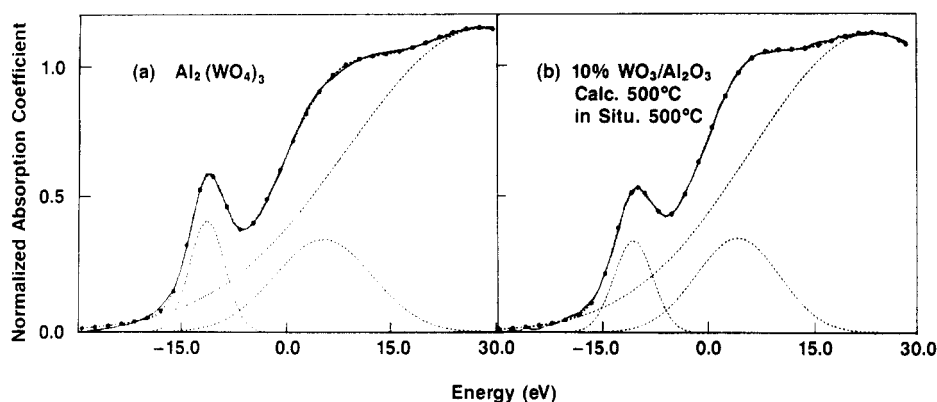(16) Kincaid, B. M.; Eisenberger, P. M. *Phys. Rev. Lett.* **1975**, *34*, 1361.
(17) Jaklevic, J.; Kirby, J. A.; Klein, M. P.; Robertson, A. S.; Brown, G. S.; Eisenberger, P. M. *Solid State Commun.* **1977**, *23*, 679.
(18) Stern, E. A.; Heald, S. M. *Nucl. Instrum. Methods* **1980**, *172*, 397.
(19) Lytle, F. W.; Greegor, R. B.; Marques, E. C.; Sandstrom, D. R.; Via, G. H.; Sinfelt, J. H., submitted to *J. Catal.*

was experimentally determined to be better than 3 cm^{-1} in cases where the spectral range was about 800 cm^{-1}. Additional details about the laser Raman apparatus can be found in ref 20.

Results and Discussion

Low Surface Coverage of WO$_3$/Al$_2$O$_3$. (a) *XANES.* Figure 1 shows the tungsten L$_1$-edge region in the crystalline reference compounds WO$_3$ and Al$_2$(WO$_4$)$_3$. The most striking difference between the spectra for the two tungsten oxide compounds is in the pre-edge region: there is a sharp, fairly intense feature in Al$_2$(WO$_4$)$_3$ and only a weak shoulder in WO$_3$. The pre-edge feature at the L$_1$ edge arises from transitions from the 2s core orbital to empty valence states that have predominantly metal d orbital character. The intensity of the pre-edge feature is determined primarily by the site symmetry of the transition-metal ion. If the ligand environment of the metal ion has octahedral symmetry, then the metal component of the upper state has d character only, and the state has gerade symmetry with respect to the center of the inversion of the octahedron. Transitions from the 2s core orbital are therefore dipole forbidden. At most a very weak quadrupole-allowed transition is observed in this case. However, if the ligand environment has tetrahedral symmetry then some p orbital character is mixed into the upper state, because of the absence of a center of inversion symmetry. In this case a well-defined, fairly intense pre-edge feature is observed, as in Al$_2$(WO$_4$)$_3$ (Figure 1a) where the WO$_4$ groups have regular and distorted tetrahedral symmetry.[15] Essentially the same XANES results were obtained with Na$_2$WO$_4$ which has the WO$_4$ group in regular tetrahedral symmetry. Any distortion of a regular octahedral environment will also remove the center of inversion symmetry and a pre-edge feature will be observed in this case, as well, although it is usually broader and less intense than the pre-edge feature for tetrahedral symmetry. The pre-edge feature for WO$_3$, where the WO$_6$ group has a distorted octahedral environment,[14] is weak (Figure 1b) and is observed only as a shoulder on the rising absorption edge.

We now compare the XANES spectra for the WO$_3$/Al$_2$O$_3$ samples, paying particular attention to the intensity of the pre-edge feature. Figure 2 shows the tungsten L$_1$-edge XANES for 10% WO$_3$/Al$_2$O$_3$ calcined at 500 °C, in the air-exposed sample at room temperature and in the same sample heated to 500 °C in an atmosphere of 20% oxygen in helium. It can be seen that there is a significant increase in the intensity of the pre-edge feature on heating to 500 °C. At this temperature the near-edge region in the 10% WO$_3$/Al$_2$O$_3$ sample strongly resembles the same region in Al$_2$(WO$_4$)$_3$, although the pre-edge peak is somewhat less prominent in the surface tungsten oxide spectrum than in the spectrum of the bulk Al$_2$(WO$_4$)$_3$ compound. The corresponding spectra for the 2% WO$_3$/Al$_2$O$_3$ sample are identical with the spectra for the 10% WO$_3$/Al$_2$O$_3$ sample shown in Figure 2. The resemblance of the WO$_3$/Al$_2$O$_3$ spectrum at 500 °C to the Al$_2$-(WO$_4$)$_3$ spectrum, where the tungsten has a tetrahedral environment, together with the lack of any change in the spectrum as the WO$_3$ loading is reduced, suggests that the surface tungsten

Figure 2. Normalized tungsten L_1-edge XANES spectra for 10% WO_3/Al_2O_3 calcined at 500 °C ($\sim^1/_3$ monolayer coverage): (a) air-exposed, room temperature sample; (b) sample at 500 °C under 20% O_2 in He.

Figure 3. Normalized tungsten L_1-edge XANES spectra for (a) $Al_2(WO_4)_3$ and (b) 10% WO_3/Al_2O_3 at 500 °C, showing the fit to three Gaussian functions (broken lines).

oxide species does consist of tetrahedral units. Cooling the WO_3/Al_2O_3 samples back to room temperature in the oxygen–helium environment did not affect the features of the XANES spectra. We attribute the difference between the spectra for the air-exposed and heated samples to the removal of coordinated water molecules.[12,13,20] Recent photoacoustic infrared studies of WO_3/Al_2O_3 have further confirmed that such a thermal treatment results in desorption of water molecules from the oxide surface.[21] The addition of two water molecules to the tetrahedral structure would produce a distorted octahedral environment for the surface tungsten oxide species, resulting in a pre-edge feature of reduced intensity. The pre-edge feature is less prominent in the heated WO_3/Al_2O_3 spectrum than in the $Al_2(WO_4)_3$ spectrum, indicating a somewhat lower oscillator strength for the corresponding core → bound state transition. Chiu et al.[22] found that an excellent fit of the Mo K edge in MoO_3/Al_2O_3 samples could be obtained using three Gaussian functions, one of which represents the pre-edge feature. We have obtained a similar fit for the tungsten L_1 edge in the WO_3/Al_2O_3 samples and the reference compounds. Figure 3 shows the fits for $Al_2(WO_4)_3$ and the in-situ 10% WO_3/Al_2O_3. The three Gaussian functions are also shown in each case. The intensity of the pre-edge feature as measured by the area of the corresponding Gaussian is about 20% lower in the heated WO_3/Al_2O_3 sample than in $Al_2(WO_4)_3$. The lower intensity of the pre-edge feature in the supported tungsten oxide can be attributed to distortion of the surface species from a regular tetrahedral structure. Wong et al.[23] found that the intensity of the pre-edge feature in a series of tetrahedrally coordinated vanadium compounds decreases significantly with increasing average

metal–ligand bond length. The distortion associated with bonding to the alumina surface could lead to an increase in the average length of the bonds to the coordinated oxygens (compared to the values in $Al_2(WO_4)_3$) and, hence, a lower intensity for the pre-edge feature.

(b) Raman Spectroscopy. The Raman spectrum of a metal oxide contains detailed structural information because the Raman vibrational modes are determined by the symmetry and structure of the coordinated compound.[24] The relationship between the metal oxide structures and the corresponding Raman vibrational spectra of several tungsten oxide reference compounds are presented below prior to discussion of the WO_3/Al_2O_3 Raman data.

Tetrahedrally coordinated molecules of the type WO_4 possess four fundamental vibrational modes, $\nu_1(A_1) + \nu_2(E) + \nu_3(F_2) + \nu_4(F_2)$, and all are Raman active. As distortions are imposed on the WO_4 structure, the symmetry is lowered and a progressively greater number of the nine, $3N - 6$, possible fundamental modes become Raman active.[24] The tungstate ion in aqueous solution, $[WO_4]^{2-}$, has been shown by Raman to have an ideal tetrahedral structure and the four fundamental modes are observed:[24] 931 cm^{-1} (A_1), 324 cm^{-1} (E), 833 cm^{-1} (F_2), and 324 cm^{-1} (F_2). Two of these bands are stretching modes (931 cm^{-1}, symmetric, and 833 cm^{-1}, antisymmetric) and two are bending modes which are degenerate in frequency at 324 cm^{-1}. Crystalline Na_2WO_4 has a spinel structure with tetrahedral site symmetry.[25] The Raman spectrum of Na_2WO_4 is shown in Figure 4 and similarly exhibits four fundamental modes of vibration at 928 cm^{-1} (A_1), 312 cm^{-1} (E), 813 cm^{-1} (F_2), 373 cm^{-1} (F_2), and a lattice vibration at 93 cm^{-1}. Crystalline $CaWO_4$ has a scheelite structure where the WO_4 group is slightly distorted from the ideal tetrahedron by compression along a line perpendicular to the two opposite edges and the site symmetry is S_4.[26] The Raman modes split due to this

(20) Wachs, I. E.; Hardcastle, F. D.; Chan, S. S. *Spectroscopy (Springfield, Oreg.)* **1986**, *1(8)*, 30.

(21) McGovern, S.; Benziger, J.; Wachs, I. E., to be submitted for publication.

(22) Chiu, N. S.; Bauer, S. H.; Johnson, M. F. L. *J. Catal.* **1984**, *89*, 226.

(23) Wong, J.; Lytle, F. W.; Messmer, R. P.; Maylotte, D. H. *Phys. Rev. B* **1984**, *30*, 5596.

(24) Nakamoto, N. *Infrared and Raman Spectra of Inorganic and Coordination Compounds*; Wiley: New York, 1978; 3rd ed.

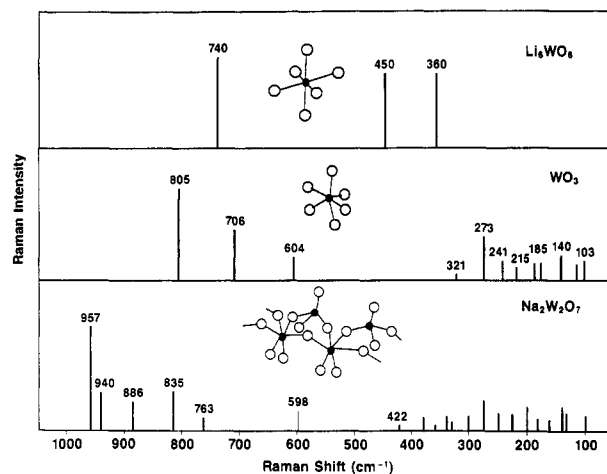(25) Busey, R. H.; Keller, Jr., O. L. *J. Phys. Chem.* **1964**, *41*, 215.

Tungsten Oxide Tetrahedral Compounds
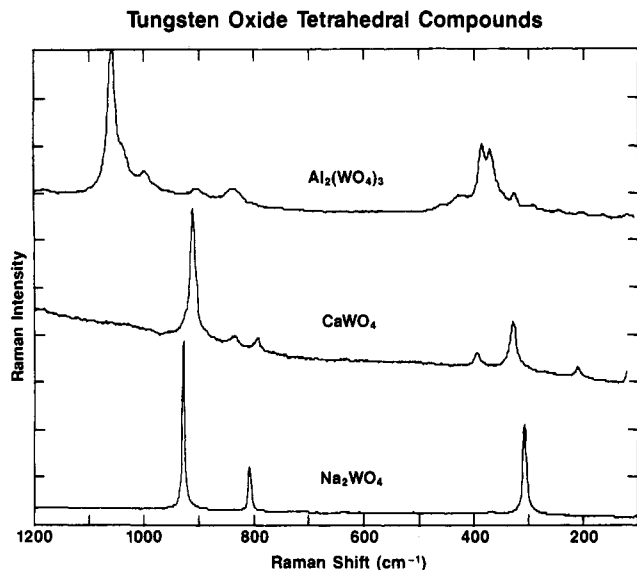
Figure 4. Laser Raman spectra of compounds possessing isolated WO$_4$ groups: Na$_2$WO$_4$, CaWO$_4$, and Al$_2$(WO$_4$)$_3$.

distortion (A$_1$ → A, E → A + B, F$_2$ → B + E), and CaWO$_4$ Raman bands are found at 922 cm^{-1} (A), 838 cm^{-1} (B), 794 cm^{-1} (E), 403 cm^{-1} (B), 334 cm^{-1} (A), 210 cm^{-1} (A), and 118 cm^{-1} (E) as shown in Figure 4. Crystalline Al$_2$(WO$_4$)$_3$ possesses a garnet structure consisting of isolated WO$_4$ tetrahedra.[14] Two different WO$_4$ groups have been identified in the Al$_2$(WO$_4$)$_3$ structure:[15] WO$_4$ tetrahedra which are regular and not significantly distorted and WO$_4$ which are distorted. The Al$_2$(WO$_4$)$_3$ Raman spectrum in Figure 4 reflects the distortion of the tungstate group and exhibits numerous Raman bands (major peaks at 1060, 387, and 372 cm^{-1}). The above tungsten oxide reference compounds only possess isolated WO$_4$ groups.

Metal–oxygen–metal (M–O–M) bonds linking two monomeric species are also identified and characterized by Raman spectroscopy. Since the transition-metal atoms are much heavier in comparison with the oxygen atoms, the isolated vibrations of the M–O–M linkage may be thought of in terms of a three-body system. Thus, there will be three fundamental vibrations expected for this system: ν_1-symmetric stretch, ν_2-bending mode, and ν_3-antisymmetric stretch. In general, for species containing a linear M–O–M bridge the antisymmetric stretch is found near 860 cm^{-1} and the symmetric stretch is near 250 cm^{-1}. For bent M–O–M linkages the antisymmetric stretch is found near 750 cm^{-1}, the symmetric stretch near 500 cm^{-1}, and the bending mode near 200 cm^{-1}.[27,28] The precise frequency depends on the mass of the metal atom. An example of a linear system is the Mo–O–Mo bridge observed for the double salt K$_2$Mo$_2$O$_7$·KBr containing binuclear ions [O$_3$Mo–O–MoO$_3$]$^{2-}$.[29] The symmetric Mo–O–Mo stretch is observed as a strong band at 501 cm^{-1} and the antisymmetric stretch is detected by infrared absorption at 835 cm^{-1} (low Raman intensity). The bent system is best exemplified by the Cr–O–Cr bridge of the dichromate ion [Cr$_2$O$_7$]$^{2-}$ in aqueous solution.[30] The antisymmetric and symmetric stretching modes are at 776 and 557 cm^{-1}, respectively; the bending mode, of much stronger intensity, is at 217 cm^{-1}. Solid K$_2$Cr$_2$O$_7$ has a Cr–O–Cr bond angle of 126° and similarly exhibits a weak symmetric stretching mode at 565 cm^{-1} and a strong bending mode at 228 cm^{-1}. The antisymmetric stretching modes are observed in IR at 795 and 759 cm^{-1}.[31] A dimeric tungsten species with a W–O–W bridge can

(26) Russell, J. P.; Loudon, R. *Proc. Phys. Soc.* **1965**, *85*, 1029.
(27) Cotton, F. A.; Wing, R. M. *Inorg. Chem.* **1965**, *4*, 867.
(28) Griffith, W. P. *Coord. Chem. Rev.* **1970**, *5*, 459.
(29) Becher, H. J.; Brockmeyer, H. J.; Prigge, U. *J. Chem. Res., M* **1978**, 1670.
(30) Michel, G.; Machiroux, R. *J. Raman Spectrosc.* **1983**, *14*, 22.
(31) Glemser, O.; Holtje, W.; Stockburger, M. *Z. Naturforsch. B* **1968**, 1137.

RAMAN SPECTRA OF TUNGSTEN (VI) OXIDE OCTAHEDRALLY-COORDINATED COMPOUNDS

Figure 5. Schematic laser Raman spectra of compounds possessing WO$_6$ groups: Li$_6$WO$_6$, WO$_3$, and Na$_2$W$_2$O$_7$.

TABLE I: Highest Wavenumber Raman Band of Tungsten Oxide Compounds

compd	wavenumber, cm^{-1}	compd	wavenumber, cm^{-1}
Octahedra		Tetrahedra	
Li$_6$WO$_6$	740	CaWO$_4$	913
WO$_3$	805	Cs$_2$WO$_4$	920
FeWO$_4$	856	Na$_2$WO$_4$	928
CoWO$_4$	886	[WO$_4$]$_{aq}^{2-}$	931
MnWO$_4$	886	BaWO$_4$	940
NiWO$_4$	893	Fe$_2$(WO$_4$)$_3$	1026
CuWO$_4$	908	Al$_2$(WO$_4$)$_3$	1060
H$_2$WO$_4$	951		
(NH$_4$)$_6$H$_2$(W$_3$O$_{10}$)$_4$	980		

be found in the peroxytungstate species K$_2$[W$_2$O$_3$(O$_2$)$_4$(H$_2$O)$_2$] where the W–O–W angle is 139°.[32] A structure based on that of the dichromate ion was proposed in which four of the doubly bonded oxygen atoms in the dichromate-type structure are replaced by four bidentate peroxide groups.[33] Raman bands were observed at 750, 556, and 250 cm^{-1} for the W–O–W antisymmetric stretch, symmetric stretch, and bending modes, respectively.[33] The corresponding dichromate frequencies are at 776, 557, and 217 cm^{-1}.[30]

Octahedrally coordinated molecules of type WO$_6$ possess only three Raman-active modes ν_1 (A$_{1g}$) + ν_2 (E$_g$) + ν_5 (F$_{2g}$).[24] As distortions are imposed on the WO$_6$ group the symmetry is lowered and a greater number of the 15 possible fundamental modes, $3N$ − 6, become active. One of the few cases in the literature of an ideal WO$_6$ octahedron is crystalline Li$_6$WO$_6$.[34] The three fundamental Raman-active vibrational modes occur at 740 cm^{-1} (A$_{1g}$), 430 cm^{-1} (E$_g$), and 360 cm^{-1} (F$_{2g}$) and are schematically illustrated in Figure 5 (reproduced from ref 34). Crystalline WO$_3$ possesses the cubic ReO$_3$ structure, the simplest three-dimensional structure formed from vertex-sharing octahedral groups. At more moderate temperatures the lattice is distorted and only at very high temperatures is the distortion removed.[14] The crystalline WO$_3$, distorted ReO$_3$ structure, Raman spectrum is schematically shown in Figure 5 and exhibits major Raman bands at 805, 706, and 273 cm^{-1}, where 805 and 706 cm^{-1} are assigned as W–O–W stretching frequencies and 273 cm^{-1} as a W–O–W bending mode.[35]

In general the position of the highest Raman band reflects the highest bond order (shortest W–O bond) present in the tungsten oxide structure.[35,36] Thus, regular tetrahedral WO$_4$ groups generally exhibit Raman bands at higher wavenumber than regular

(32) Einstein, F. W. B.; Penfold, B. R. *Acta Crystallogr.* **1964**, *17*, 1127.
(33) Griffith, W. P. *J. Chem. Soc.* **1963**, 5345.
(34) Hauck, J.; Fadini, A. *Z. Naturforsch. B* **1970**, *25b*, 422.
(35) Beattie, I. R.; Gilson, T. R. *J. Chem. Soc. A* **1969**, 2322.
(36) Knee, F.; Condrate, Sr., R. A. *J. Phys. Chem. Solids* **1979**, *40*, 1145.

octahedral WO_6 groups because of their higher bond order (shorter W–O bond). Distortions in the tetrahedral WO_4 and octahedral WO_6 groups, however, can give rise to very significant increases in the W–O bond order of both structures which complicate the distinction between WO_4 and WO_6 groups based on band position. Table I lists a series of tungsten oxide compounds with tetrahedral and octahedral coordinations and their highest wavenumber Raman bands. The octahedra possess Raman bands between 740 and 980 cm^{-1} and the tetrahedra possess Raman bands between 913 and 1060 cm^{-1}. There is much overlap in the band positions of the octahedral and tetrahedral tungsten oxides, but only the octahedra have bands below about 910 cm^{-1} and only the tetrahedra have bands above about 980 cm^{-1}. As an extreme case, ammonium metatungstate possesses WO_6 octahedra of significant distortion, and the symmetric stretch appears at about 980 cm^{-1}. For less-distorted octahedra the stretch would be expected at lower wavenumbers. Therefore, in order to adequately differentiate between tungsten oxide tetrahedral and octahedral species by using the symmetric stretch as a rough guideline, only the extreme regions of the spectrum, i.e., below 910 and above 980 cm^{-1}, may be utilized. If the stretch occurs within the overlap region, i.e. 910–980 cm^{-1}, an attempt at vibrational mode analysis must be made, either by analogy with known standards or by computation.

The above discussion centered on tungsten oxide compounds having either a tetrahedral or an octahedral coordination. A structure that possesses both octahedral and tetrahedral tungsten oxide groups is disodium ditungstate, $Na_2W_2O_7$. The $Na_2W_2O_7$ structure is composed of WO_4 and WO_6 units joined in infinite chains.[36,37] The tungsten oxide octahedra share corner oxygen atoms with adjacent octahedra and are also attached to tungsten oxide tetrahedra; the tungsten oxide tetrahedra share oxygen atoms with two different adjacent tungsten oxide octahedra in the chain. The Raman spectrum of $Na_2W_2O_7$ is schematically illustrated in Figure 5 (reproduced from ref 36). The Raman bands at 957 and 940 cm^{-1} are assigned to symmetric W–O stretching modes of the WO_4 tetrahedra and the bands at 835, 763, and 598 cm^{-1} are assigned to W–O stretching modes of the WO_6 octahedra.[36] The remaining bands can be assigned to bending modes, and the strong bending modes at 200–300 cm^{-1} reflect the W–O–W bonds in this infinite chain structure. Although the $Na_2W_2O_7$ structure is composed of an equal concentration of tungsten oxide tetrahedra and octahedra, the WO_4 tetrahedra dominate the $Na_2W_2O_7$ Raman spectrum and the WO_6 octahedra give rise to much weaker bands. The stronger Raman signal from the WO_4 tetrahedra is related to the higher bond order present in the tetrahedral structure than the octahedral structure of $Na_2W_2O_7$.[37] Thus, structures simultaneously possessing tungsten oxide tetrahedra and octahedra will generally produce a Raman spectrum that is dominated by the tungsten oxide tetrahedra.

The above Raman assignments are now used to interpret the Raman spectra of the supported tungsten oxide on alumina. The Raman spectra of 2% and 10% WO_3/Al_2O_3 calcined at 500 °C are presented in Figure 6. Both samples exhibit Raman bands at 970–990 and 880–910 cm^{-1} as well as very broad bands at 200–400 cm^{-1}. The broad Raman bands at 200–400 cm^{-1} appear to be composed of two overlapping bands centered at 250 and 325 cm^{-1}. The Raman band at 250 cm^{-1} is consistent with the presence of a W–O–W linkage as was discussed earlier. The W–O–W bond would also be expected to exhibit very weak antisymmetric and symmetric stretches in the 700–800- and 500–600-cm^{-1} regions, respectively. A close examination of the 10% WO_3/Al_2O_3 sample reveals a very weak Raman band between 500 and 600 cm^{-1} that is just detectable above the background. The antisymmetric W–O–W stretch at 700–800 cm^{-1} would be expected to be even weaker than the symmetric stretch and would not be detectable above the background. Dehydration of these samples causes the maximum Raman bands to shift to 1010–1030 cm^{-1}.[12,13] Such a high wavenumber position for the tungsten–oxygen stretch suggests that W=O bonds are present in the surface tungsten
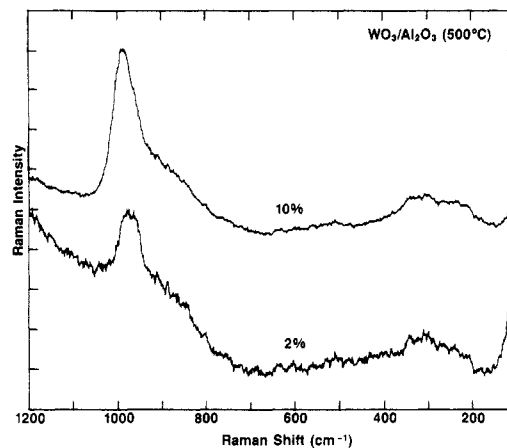

Figure 6. Laser Raman spectra of WO_3/Al_2O_3 calcined at 500 °C as a function of tungsten oxide content.

oxide complex, and that the structure most likely consists of a distorted, tetrahedral coordination (see Table I). The observed Raman bands at 970–990, 880–910, and 325 cm^{-1} are consistent with a distorted WO_4 structure (the Raman spectrum of Na_2WO_4, which contains a regular tetrahedral tungstate, exhibits the corresponding Raman bands at 928, 813, and 312 cm^{-1}). The presence of some surface tungsten oxide octahedra in these samples cannot be addressed by Raman spectroscopy alone because of the low Raman scattering efficiency of such a structure, but the earlier XANES measurements revealed that, in the absence of moisture, the surface tungsten oxide possesses tetrahedral coordination.

The absence of tungsten oxide octahedra is demonstrated by the XANES data. The XANES and Raman results both suggest that the surface tungsten oxide complex on alumina (<1/3 monolayer) possesses a distorted tetrahedral structure. The Raman results also provide evidence for the presence of W=O and W–O–W bonds in the surface tungsten oxide on alumina. These observations are consistent with tetrahedral-coordinated tungsten oxide where a fraction of the species are in a dimeric form:
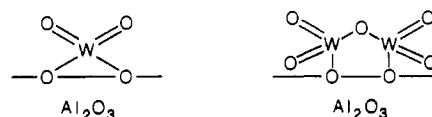

In the presence of moisture the water molecules coordinate to these tetrahedral structures to produce distorted octahedral environments. The water coordination is reflected in the reduced intensity of the XANES pre-edge feature and a shift of the symmetric stretch of the Raman band to lower wavenumber.

High Surface Coverage of WO_3/Al_2O_3. Although the XANES spectra of alumina-supported tungsten oxide samples with a low surface coverage (<$^1/_3$ monolayer) suggest a distorted tetrahedral structure for the surface species, the situation changes as the coverage approaches one monolayer. Figure 7 shows the tungsten L_1 XANES for a 10% WO_3/Al_2O_3 sample calcined at 950 °C, both air-exposed at room temperature and in-situ at 500 °C. The 950 °C calcination treatment collapses the surface area of the Al_2O_3 support from 180 to ~65 m^2/g and produces a coverage of about one monolayer of the surface tungsten oxide species.[7] In this case the XANES spectrum of the air-exposed WO_3/Al_2O_3 sample strongly resembles the spectrum of the same region in the bulk WO_3 reference compound and indicates that a significant fraction of the surface tungsten oxide species have distorted octahedral coordination. There is a small increase in the intensity of the pre-edge feature of the 950 °C calcined 10% WO_3/Al_2O_3 sample upon dehydration by heating to 500 °C, but the feature is still significantly less prominent than that in the spectrum of the 10% WO_3/Al_2O_3 sample calcined at 500 °C. L_1-edge spectra almost identical with those in Figure 7 were obtained for a 30% WO_3/Al_2O_3 sample calcined at 500 °C, where the coverage was also approximately one monolayer.[5,7,8] We infer that at monolayer

(37) Okada, K.; Morikawa, H.; Marumo, F.; Iwai, S. *Acta Crystallogr., Sect. B* **1975**, *B31*, 1200.
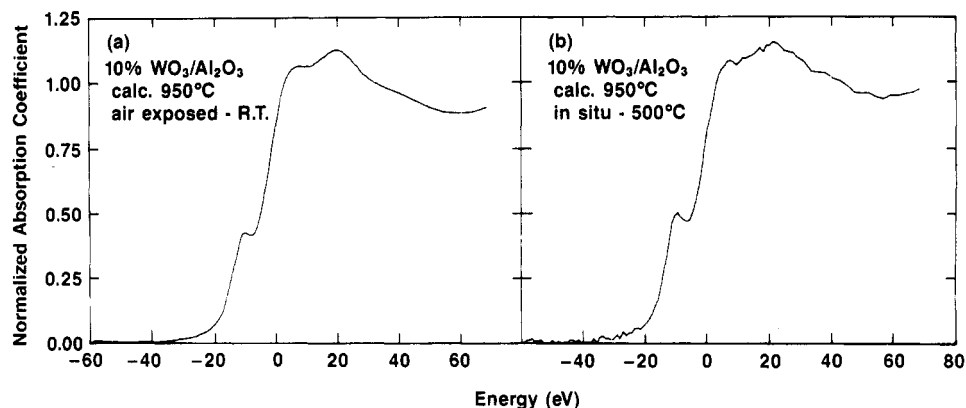
Figure 7. Normalized tungsten L$_1$-edge XANES spectra for 10% WO$_3$/Al$_2$O$_3$ calcined at 950 °C ($\sim$1 monolayer coverage): (a) air-exposed, room temperature sample; (b) sample at 500 °C under 20% O$_2$ in He.
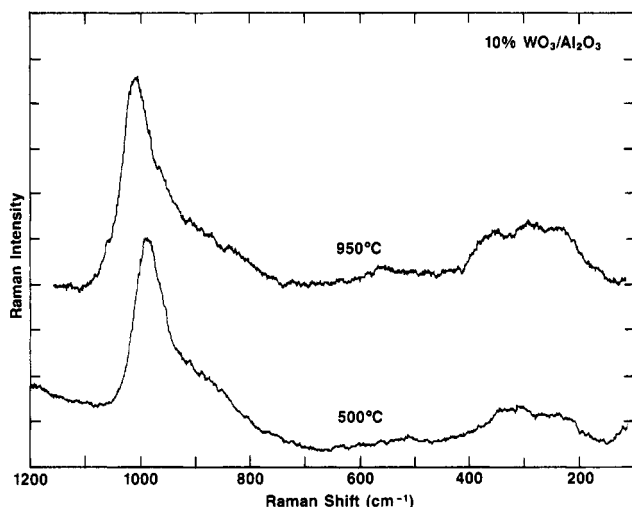
Figure 8. Laser Raman spectra of 10% WO$_3$/Al$_2$O$_3$ as a function of calcination temperature.

surface coverage of tungsten oxide a significant fraction of the sites have a distorted octahedral environment even when the coordinated water molecules have been removed.

The Raman spectrum of the 10% WO$_3$/Al$_2$O$_3$ sample calcined at 950 °C is shown in Figure 8. Additional Raman bands due to the phase transformation of γ-Al$_2$O$_3$ (Raman inactive) to θ-Al$_2$O$_3$ (Raman active) have been subtracted from the spectrum for the sake of clarity.[7,8] The most intense Raman band of the surface tungsten oxide shifts from 986 to 1001 cm^{-1} after the 950 °C calcination. This reflects the formation of a close-packed monolayer of tungsten oxide on alumina as the support area decreases.[7] Dehydration of this sample causes the major Raman band to shift to $\sim$1010–1030 cm^{-1}[12,13] and reflects the presence of tetrahedral surface tungsten oxide possessing W=O bonds. The Raman bands that we have attributed to W–O–W bonds become more pronounced at $\sim$250 and 500–600 cm^{-1}, indicating a higher concentration of W–O–W linkages at the higher coverage. No other significant changes are observed between the Raman spectra of 10% WO$_3$/Al$_2$O$_3$ calcined at 500 and 950 °C (see Figure 8). The Raman insensitivity toward the octahedral tungsten oxide component in the 10% WO$_3$/Al$_2$O$_3$ (950 °C) sample, whose presence was detected by XANES, is due to the lower Raman cross section of the WO$_6$ octahedra than the WO$_4$ tetrahedra, as was earlier observed for crystalline Na$_2$W$_2$O$_7$ (composed of infinite chains of attached WO$_6$ and WO$_4$ units). Thus, for the 10% WO$_3$/Al$_2$O$_3$ sample calcined at 950 °C, the Raman spectrum is overshadowed by the tetrahedral component of the surface tungsten oxide.

The XANES results suggest that at monolayer surface coverage of tungsten oxide a significant fraction of the sites have a distorted octahedral environment even after dehydration by heating to 500 °C. The corresponding Raman results are overshadowed by the

tetrahedral component and show evidence of W=O and W–O–W bonds in the tetrahedral fraction of the surface tungsten oxide monolayer on alumina. These observations are consistent with a surface complex where the supported tungsten oxide has formed a polymeric structure on the alumina support composed of WO$_4$ and WO$_6$ units joined in infinite chains. The strong affinity for tungsten oxide to form extensive W–O–W bonded structures rather than isolated tungsten oxide structures is well documented in the literature.[14] The crowding of the surface tungsten oxide on the alumina support at monolayer coverage apparently allows for the extensive formation of the W–O–W bonds and the chainlike surface structure.

Earlier characterization studies of the WO$_3$/Al$_2$O$_3$ system found that the reducibility of the surface tungsten oxide species on alumina is a function of the surface coverage of the tungsten oxide phase.[2,11] At low coverages, the surface tungsten oxide species is not reducible even in flowing hydrogen at 900 °C for 2 h.[11] At coverages approaching a monolayer, approximately half of the surface tungsten oxide is reduced to metallic tungsten with the same treatment.[11] The current findings that the coordination of the surface tungsten oxide on alumina varies with coverage may account for the reducibility trends of WO$_3$/Al$_2$O$_3$. At low coverages, the surface tungsten oxide is present as isolated and dimeric tetrahedra that apparently are extremely difficult to reduce. As monolayer coverage is approached, a significant fraction of the surface tungsten oxide possesses an octahedral environment which appears to be responsible for the reduction at these conditions. The structure–reduction correlation for the WO$_3$/Al$_2$O$_3$ system nicely demonstrates how the chemical properties of a supported metal oxide phase depends on the molecular structure of the surface species.

Conclusions

In summary, the XANES spectra of the L$_1$ tungsten edge in WO$_3$/Al$_2$O$_3$ samples indicate that the symmetry of the tungsten environment depends on both the surface coverage and the presence of coordinated water. At coverages of less than $^1/_3$ monolayer in the absence of coordinated water the spectrum indicates a distorted tetrahedral structure for the surface species. Samples exposed to air at room temperature have water molecules coordinated to some fraction of the sites, producing an octahedral site symmetry, but the water is removed by heating to 500 °C. Laser Raman spectra of the WO$_3$/Al$_2$O$_3$ samples are consistent with a distorted tetrahedral tungsten environment and, in addition, show features that can be attributed to W=O and W–O–W bonds. We propose that the surface tungsten oxide on alumina is present as both isolated and dimeric tetrahedra, in order to explain these results. At coverages approaching a monolayer, however, the changes in the near-edge region associated with the removal of the water molecules were much less evident than at low coverage. At high coverage a significant fraction of the surface tungsten sites appear to have a distorted octahedral environment even after dehydration by heating to 500 °C. The corresponding Raman results are overshadowed by the tetrahedral component

and show evidence of W=O and W-O-W bonds in the tetra-hedral fraction of the surface tungsten oxide monolayer on alumina. These observations are consistent with a surface complex where the supported tungsten oxide has formed a polymeric structure on the alumina support composed of WO_4 and WO_6 units joined in infinite chains. The current study demonstrates for the first time the powerfulness of combining XANES and Raman spectroscopy in structural studies of supported metal oxide systems.

Surface Properties of Carboxylate Latex Particles

P. Baglioni,* R. Cocciaro, and L. Dei

Department of Chemistry, University of Florence, 50121 Firenze, Italy (Received: November 10, 1986; In Final Form: February 23, 1987)

The interfacial properties of a styrene–butadiene–acrylic acid polymeric latex and their variation by the addition of a surfactant, sodium dodecyl sulfate (SDS), able to be adsorbed at the latex interface, were studied by means of the ESR spectroscopy of nitroxide probes. The parameters analyzed in this study were the nitrogen coupling constant, $\langle A_N \rangle$, the correlation time, τ, and the ESR line shape. We have demonstrated that the latex interface presents, to a foreign molecule that can interact with the latex, two different "sites" of interaction: apolar sites directly exposed to the solvent interaction and polar sites mainly located in the water phase. The addition of SDS decreased the exposition of the latex hydrophobic polymeric chains to the solvent only for high latex surface coverage (more than 70%), indicating that the latex "stabilization" can occur only when its interface is nearly fully covered by SDS molecules. The ESR spectra obtained for high SDS concentrations added to the latex indicated that SDS micelles and latex particles, fully covered by SDS monomers, coexisted in solution.

Introduction

Monodisperse latices are of fundamental importance both from a theoretical and from a practical point of view. In fact, they have represented and still represent the first choice model for testing theories about the colloidal stability.[1] Furthermore, the industrial applications of these compounds are increasing and require that these compounds have different specific properties, such as a particular surface groups for improved colloid stability, and/or interactions with particular substrates.

Considering the above, many studies have been reported in the literature regarding the "surface characterization". The principal aim is the determination of the concentration and strength of the acid or basic groups present at the latex interface, which are mainly responsible for the stability and, in some cases, for the properties of the latices themselves.[2-6] Further, the possibility of modifying the surface of the latices and some of their physicochemical properties by adsorption of surfactants makes these systems very attractive for the study of the relationships between the physicochemical properties of the adsorbate and that of the latex.[7-9]

In previous studies on micellar systems we showed that it is possible to obtain information on different regions of the micellar interface by using spin probes that can interact in different ways with micelles. Generally, "hydrophilic" spin probes give information on solvation layers of the micellar interface,[10] whereas spin probes bearing a "hydrophobic" chain give information on the micellar surface.[11]

TABLE I

composition, %	
styrene	59
butadiene	38.9
acrylic acid	1.1
concentration, %	4.24
pH	4.6
av particle diam, Å	1400 (monodispersed)
surface tension, dyn/cm	68.3
carboxyl groups	$16/1000$ Å^2
sulfate groups	$5/1000$ Å^2 (from initiator)

In this study we followed a similar approach and we applied, for the first time as far as we know, ESR spectroscopy to the study of the latex interface and its modification by adsorption of a surfactant (sodium dodecyl sulfate (SDS)). We showed that the application of this spectroscopy, together with the classical adsorption isotherms, can give very useful information.

In particular, two different spin probes were used: the cationic probe 4-trimethylammonium-2,2,6,6-tetramethylpiperidine-1-oxyl iodide (Temp-TMA+), able to interact with the anionic groups present at the latex surface and with the polar headgroups of the added surfactant, and the nonionic octanoyloxy-2,2,6,6-tetramethylpiperidinyl-1-oxy (C8-TEMPO) that can interact with the polymeric hydrophobic chains of the latex and of the surfactant present at the latex interface.

The ESR parameters analyzed in this study were (a) the correlation time for the probe motion, τ, related to the microviscosity of the probe environment; (b) the nitrogen hyperfine coupling constant, $\langle A_N \rangle$, related to the dielectric constant of the medium, to the Kosower factor, and to the medium polarity; and finally (c) the ESR line shape, which gave information about the probe chemical exchange among different chemical sites present at the latex interface.

Experimental Section

The latex used in this study (styrene–butadiene–acrylic acid) was a gift from Enichem Elastomeri, Milano. It was cleaned by

(1) Buscall, R.; Ottewill, R. H. In *Polymer Colloids*; Buscall, R., Corner, T., Stageman, J. F., Eds.; Elsevier: New York, 1985; pp 141–217, and references therein.

(2) Labib, M. E.; Robertson, A. A. *J. Colloid Interface Sci.* **1980,** *77,* 151.

(3) Van Den Hull, H. J.; Vanderhoff, J. W. *J. Electroanal. Chem.* **1972,** *37,* 161.

(4) Hen, J. *J. Colloid Interface Sci.* **1974,** *49,* 425.

(5) Ottewill, R. H.; Shaw, J. N. *Kolloid Z. Z. Polym.* **1966,** *234,* 34.

(6) Shirahama, H.; Suzawa, T. *J. Appl. Polym. Sci.* **1984,** *29,* 3651.

(7) Piirma, I.; Chen, S. R. *J. Colloid Interface Sci.* **1980,** *74,* 90.

(8) Kronberg, B.; Stenius, P. *J. Colloid Interface Sci.* **1984,** *102,* 410.

(9) Kronberg, B.; Stenius, P.; Igeborn, G. *J. Colloid Interface Sci.* **1984,** *102,* 418.

(10) Ottaviani, M. F.; Baglioni, P.; Martini, G. *J. Phys. Chem.* **1983,** *87,* 3146. Baglioni, P.; Ottaviani, M. F.; Martini, G. In *Surfactants in Solution*; Mittal, K. L., Lindman, B., Eds.; Plenum: New York, 1984; Vol. 1, pp 541–557. Baglioni, P. In *Surfactants in Solution*; Mittal, K. L., Bothorel, P., eds.; Plenum: New York, 1986; Vol. 4 pp 393–404.

(11) Baglioni, P.; Ferroni, E.; Martini, G.; Ottaviani, M. F. *J. Phys. Chem.* **1984,** *88,* 5107. Baglioni, P.; Ottaviani, M. F.; Martini, G. *J. Phys. Chem.* **1986,** *90,* 5878.